77th IIW Annual Assembly and International Conference on Welding and Joining 7-12 July 2024 Rhodes, Greece

The effect of welding and strain conditions on the susceptibility to solidification cracking of a fully austenitic stainless steel

Shaowei Yang[1], Tamaki Ito[1], Kenji Shinozaki[1] , Motomichi Yamamoto[1]

[1] Graduate School of Advanced Science and Engineering, Hiroshima University, Japan

Abstract. Solidification cracking is a commonly welding defect, especially in high-sulfur steels, austenitic steels, and nickel-based superalloys. It becomes a serious problem when various materials and fastest welding speed are recommended to increase productivity. Conventional solidification cracking test equipment exposed limitation in obtaining high temperature ductility curves precisely for cracking evaluation. This research developed an in-plain constraint and relaxation type system for evaluation of solidification cracking. Type 310S austenitic stainless steels was selected as testing material to investigate the effect of welding and strain conditions on susceptibility to solidification cracking. Lower initial loads that required for starting crack exhibited in the weldment with increase of welding speed. While ductility curves did not show significant change when increasing welding speed. In addition, the width of specimen was decreased to change the strain rate, and thus the flexibility of developed system was verified. The proposed technique in the present study has proven to obtain the critical strain more precisely than previous testing methods.

1 Introduction

Stainless steels were known to have excellent resistance to corrosion, creep, and high temperature oxidation [1]. Thus, they are considered as ideal technique candidates for a variety of applications such as fuel tanks in rocket components, automotive body materials, medical equipment, structural materials for pressure vessels [2]. However, cracking problems faced during manufacturing or application, such as solidification cracking in welding, or hot tearing in casting [3]. Among these, austenitic stainless steels are prone to crack because it's low solubility of impurity elements such as sulfur and phosphorous that prone to segregate into eutectic liquid films deteriorating strength of inter-dendritic regions during solidification. This indicates more susceptible to solidification cracking for austenitic stainless steel, even they were accepted by a variety of applications.

Solidification cracking forms at a mushy zone which is the semisolid region located between the moving molten pool and the completely solidified weld metal. Figure 1a-b shows the schematic illustration of solidification process during welding. The mushy zone is surrounded by two isothermal surfaces corresponding to liquidus temperature (T_L) and solidus temperature (T_S). In welding, columnar dendritic grains are usually dominant in the mushy zone unless grain refining is conducted [1]. During solidification and cooling, the mushy zone tends to contract due to solidification shrinkage and thermal contraction. However, this free contraction would be obstructed due to the connection to the rigid workpiece that is much cooler and larger in sizes, thus inducing tension to separate columnar grains, and probably cause cracking [4]. In addition, as shown in Figure 1c, during solidification, the ductility of materials drops down dramatically in the mushy zone. Solidification cracking occurs when a high temperature strain generated in the mushy region behind a molten pool exceeds the ductility of weld metal within the solidification temperature range [5-6].

The evaluation method for susceptibility to solidification cracking was investigated. Prokhorov [7] established high temperature ductility curves to illustrate solidification cracking susceptibility by defining the minimum ductility required for cracking occurrence. As shown in Figure 1c, the susceptibility to solidification cracking can be evaluated by the intersection of the high temperature ductility curve and the critical strain history curve. It is believed that the brittleness temperature range (BTR) in ductility curve is highly related to the solidification cracking, that is, the lager the BTR, the greater likelihood to crack [8]. Yoshiaki et al. [9] compared the brittleness temperature range of austenitic stainless steels according to content elements. Wang et al. [10] also investigated the susceptibility to solidification cracking by measuring brittleness temperature range according to the welding speed during laser welding. The BTR of various materials and the relationship between different conditions and BTR were investigated, which implies the important role of this index. Solidification cracking will occur only when the critical strain intersects with high temperature ductility curve of materials in the brittleness temperature range. However, there are few studies and methods to consider the critical strain curve in previous research.

Shinozaki et al. [11] developed U-type hot cracking test with in-situ observation to measure the critical strain history curve. In this test, the specimen used for testing is welded by laser while being stretched normal to the welding direction by transverse tensile load to create crack. A high-speed camera is applied to record the real of the molten pool to calculate the critical strain by in-situ image analysis. The U-type hot cracking test was widely used for the evaluation of solidification cracking. However, it has been pointed out that there are some difficulties for observing and assessing solidification

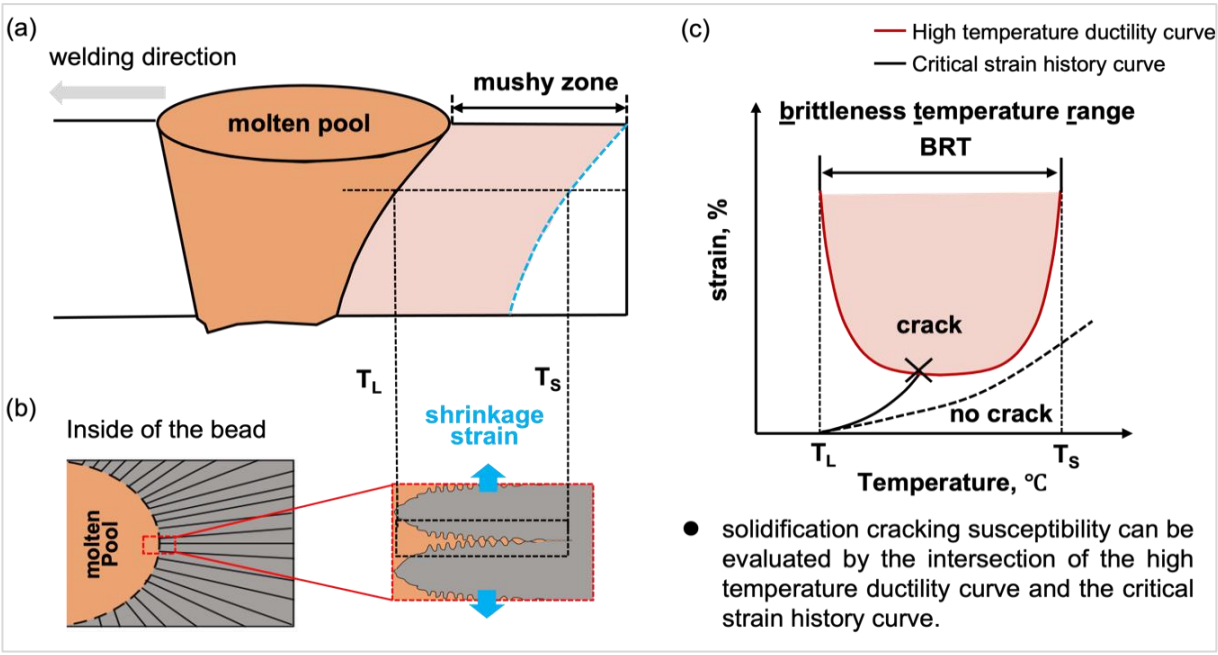

Figure 1. Schematic illustration of the solidification cracking: (a) view of molten pool and the mushy zone during solidification; (b) surroundings of columnar grains during solidification; (c) illustration of evaluation method for solidification cracking susceptibility.

cracking due to low-quality in-situ imaging and complex strain type during welding [12-13]. Thus, the conventional testing equipment for evaluating hot cracking susceptibility has relatively low repeatability and low accuracy. Moreover, the thickness of the specimen greatly affects the accuracy of the results. Because the crack generally starts inside the material and gradually extends to the surface observed by the camera during the hot cracking test. Therefore, a novel hot cracking test system, with high imaging quality, high accuracy applicable to thinner plates to obtain reliable accurate high-temperature strain curve is highly desirable.

This study proposed a novel hot cracking test equipment, called in-plain constraint and relaxation type cracking test, for evaluating solidification crack of type 310S stainless steel at different welding speed and strain conditions. An in-situ observation technique, which was developed and verified by previous studies [14-15] was carried out to measure the critical strain history during the hot cracking test. In addition, objective lens was firstly attached to the high-speed camera to obtain in-situ imaging with high magnification during laser welding. Then, the ability of developed system and hot cracking test result during welding were discussed.

2 Experiment procedure

2.1 Materials, welding conditions and new test method.

The specimen of type 310S stainless steel with a thickness of 1 mm, a width of 80 mm and a length of 110 mm was used for the hot cracking test. The chemical composition of the material is shown in Table 1. To investigate the details of cracking occurrence and calculate the critical strain precisely, a new-type testing system was developed, as shown in Figure 2. Fiber laser was used as a heat source. The laser power of 1.1 kW, 1.7 kW and 2.5 kW for welding speed of 0.3 m/min, 0.6m/min, and 0.9 m/min, respectively. Ar gas with a flow rate of 50 L/min was used as shielding gas to prevent oxidation at the weld region during the laser welding.

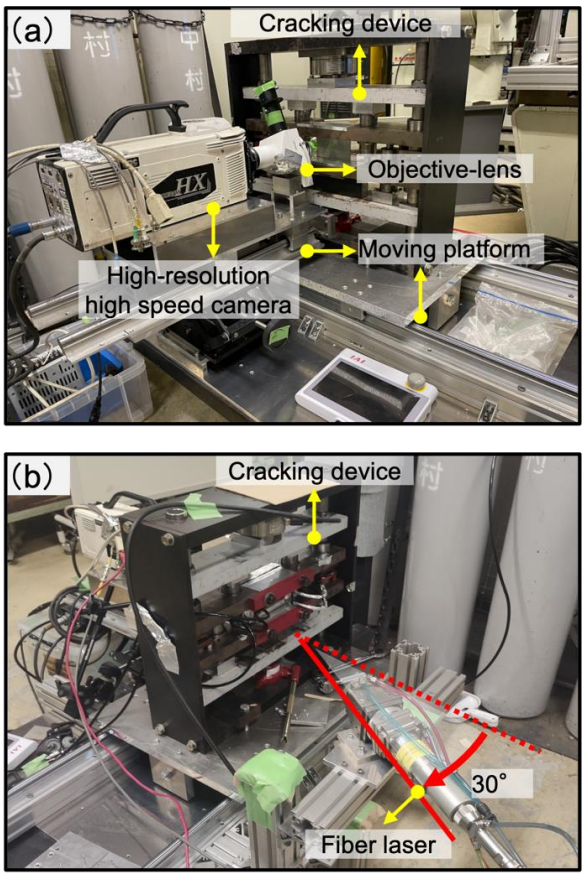

Figure 2. The solidification cracking test system: (a) observation side using high speed camera; (b) laser side setup appearance.

Table 1 Chemical composition of Type 310S stainless steel.

Material	Chemical composition, mass%								
	C	Si	Mn	P	S	Ni	Cr	Co	Fe
SUS310S	0.04	0.43	0.96	0.019	0.001	20.13	25.19	0.09	Bal.

Table 2 Welding conditions.

Welding speed, m/min	**0.3**	**0.6**	**0.9**
Laser power, kW	1.1	1.7	2.5
Defocus length, mm	28.3		
Laser irradiation angle, deg	30		
Shape of penetration	Full penetration		
Ar shielding gas, L/min	50 (front and back side)		

It is well knowing the importance to obtain solidification cracks with different loading force to obtain the critical strain for crack initiation. Figure 3 shows the schematic illustration of new developed hot cracking test equipment. This equipment mainly consists of four springs, two grippers, one jack and load cell in its body. The loading force can be applied by the Jack and evenly transfers to the specimen through the Die springs and Grippers which makes a controllable linear force possible. Moreover, by using springs of different stiffness, the strain rate produced during welding can be varied flexibly for the hot cracking test. It should be noted that this equipment enables thinner plates for the test to decline the time delay of crack transmission to the observation surface, which improve the accuracy of results.

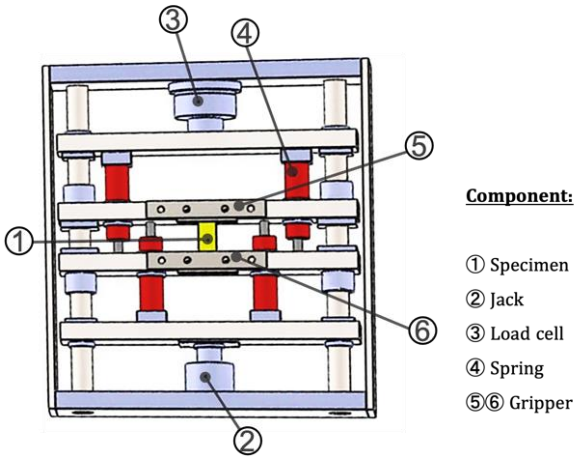

Figure 3. Schematic illustration of hot cracking test equipment

2.2 Measurement of critical strain for cracking initiation

The high-speed camera with high-resolution attached with the objective lens is combined with the device to obtain the high-magnified and clear in-situ images of solidification cracking with many flexibilities. As shown in Figure 2, imaging is performed from the back of the specimen to avoid laser fumes, spatters, etc. Table 3 indicates the shooting conditions for the observation of cracking occurrence and strain measurement by in-situ observation method. The high-speed camera was attached with a short pass filter (725nm) for preventing laser directly entering the image sensor. Then, the critical strain for the cracking occurrence was measured from the images captured by the camera using the Dipp-MotionPRO2D software. As shown in Figure 4, once the solidification cracking was found initially from the image, two reference points were chosen along the tensile direction and the distance between two points at t_C was measured as Lc. The reference points can be continuously tracked by rewinding the video to the moment ($t=t_0$) when the welding pool edge forms by solidification. Then, the distance between two reference points at t0 was measured as L0. Thus, the time dependent strain rate can be calculated by Eq. (1):

$$\varepsilon = \frac{Lc - L_0}{L_0} X\ 100\ (\%) \qquad (1)$$

Table 3 Shooting conditions

Camera	High-speed camera
Lighting	LED
Lens	Objective lens
Resolution, pixel	2560×1920
Frame rate, fps	500
Shutter speed, sec	200k
Lens magnification, μm	2.15
Optical filter	Short-pass filter (725nm)

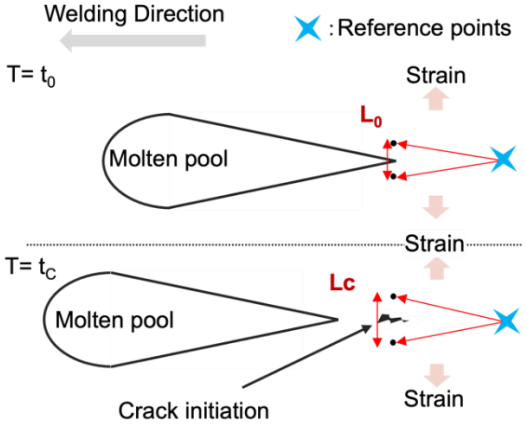

Figure 4. Schematic illustration of measurement method for critical strain of solidification cracking

3 Results and discussion

3.1 Hot cracking test results

Figure 5 shows cracking test results at different welding speed. For more easier comparison, the welding conditions at a welding speed at 0.1 m/min was also introduced to the experiment. The samples without cracking occurrence were represented with blue circle, while cracking samples with red cross. No cracks occurred for all samples at welding speed of 0.1 m/min. The critical initial loads for cracking occurrence 16.34 kN, 11.93 kN, 7.69 kN for welding speed of 0.3 m/min, 0.6 m/min, 0.9 m/min respectively. During welding, the weld metals were subjected to different degrees of tensile in-plain strains transverse to the welding direction at various initial load conditions. When adequate strains accumulated in the mushy zone that is susceptible to solidification exceeds the strength to separate the liquid film, cracks would be occurred. This indicates lower initial loads for creating a crack led to higher cracking susceptibility.

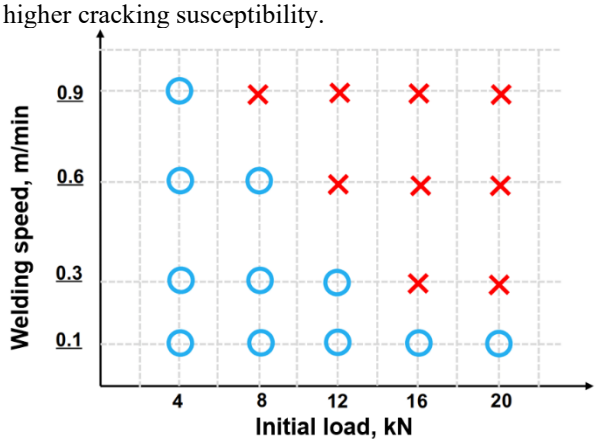

Figure 5. Hot cracking test result

3.2 Obtaining critical strains for cracking occurrence

The high-speed camera with high resolution and objective lens was used to observe the crack initial occurrence during the solidification. Figure 6 shows typical example of the captured solidification cracking images during the laser welding with high magnification lens of ×10 (1.10 μm/pixel). These images were presented through the treatment of video upend to observe the initiation of solidification cracking occurrence. It should be noted that observation from different side with laser provided a stable condition without the negative effect of reflected laser beam and fumes. The broken line in Figure 6 represents the liquid and solid interface determined from the in-situ observation images.

In this study, the microstructure formation during melting and cracking process was clearly observed. Solidification cracking was observed generated at the rear of the molten pool and continuously propagated along the centrelines of weld bead to the welding direction. It has been proved that the initiation of solidification cracking could be clearly recognized because cracking disappeared at that moment, as indicated by yellow arrow in Figure 6. Therefore, it is expected that the disadvantages of the conventional testing.

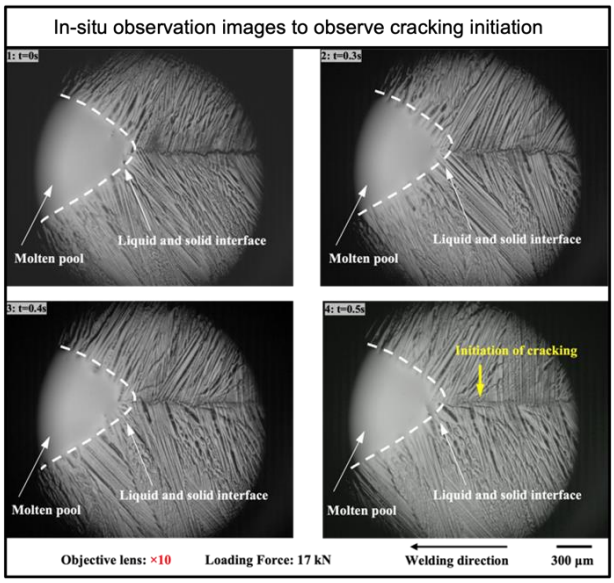

Figure 6. Solidification cracking images obtained by high magnified in-situ observation technique (after the treatment of video upend)

Once the initial cracking moment recognized by in-situ observation method motioned above, the critical strain as well as strain histories curves can be calculated. The method for calculation was displayed in 2.2 section. Figure 7 shows one of results of strain histories at welding speed of 0.3 m/min. Note that this result shows row data obtained from in-situ observation without any treatment. Less dispersion of stain history curves indicates high precision of developed system in present works.

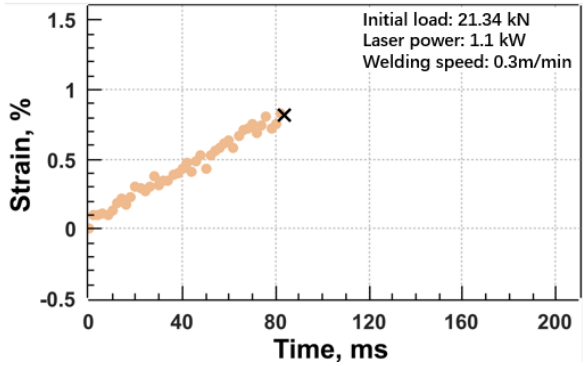

Figure 7. Solidification cracking images obtained by high magnified in-situ observation technique (after the treatment of video upend)

3.3 Temperature measurement during welding

A noncontact measurement method for temperature was introduced to this work. This method was developed in our previous studies. Figure 8 shows the temperature measurement result at the welding speed of 0.3 m/min. The horizontal axis displays the distance from the molten pool to the mushy zone. The liquid temperature was recognized as 1424 ℃ through temperature profile measured by in-situ observations. The brittleness temperature range was obtained by using Tran-varestraint test in our previous works. Brittleness

temperature range was calculated as 102℃ and showed constant in the range of 0.3 m/min to 0.9 m/min. That means the residual liquid in the mushy zone not changed significantly according to the welding speed. This work based on our previous works and check the ductility curves at each welding speed conditions.

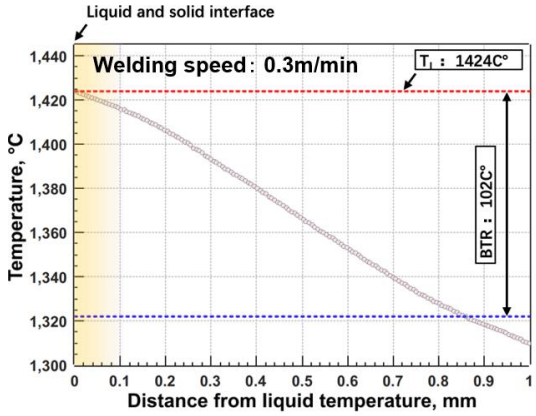

Figure 8. Temperature measurement result of SUS310S at welding speed of 0.3 m/min

3.4 High temperature ductility curves

Figure 9 shows obtaining high temperature ductility curves combining both thermal-crtitical strain histories curves and temperature measurement results. Each points represents critial strains for requiring cracking initial occurrence at different loading conditons. Alough lower initial loads for starting crack, the obtained ductility curved did not showed significant change in this study.

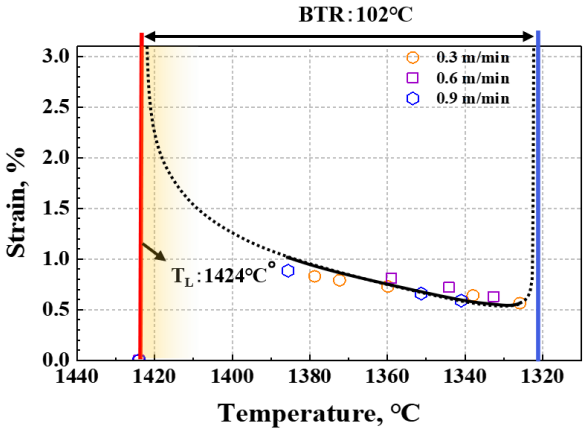

Figure 9. The high temperature ductility curves obtained at different welding speeds.

4 Conclusions

1. A new hot cracking test system based on the in-situ observation technique has been developed and used to observe the cracking occurrence and measure critical strain history curves with high precision.
2. In the present test, type 310S stainless steels are welded by the laser at different welding speed. The test is useful because the tensile strain type that stretched to the mushy zone to cause solidification cracking is simper liner strain compared with widely used U-type test.
3. Lower critical initial load for cracking occurrence with increase of welding speed from 0.3 m/min to 0.9 m/min, indicating a higher tendency for cracking.
4. A non-contact temperature measurement method was proposed here to measure the temperature profile behind the welding pool followed by combinations of strain histories curves and temperature curves.
5. High temperature ductility curves were obtained and did not show significant changes at different welding speed from 0.3 m/min to 0.9 m/min.

References

1. Koseiki. Toshihiko, Inoue. Hiroshige, et.al., Nippon Steel Technology Report., No. 65, April 1995.
2. K. Liu, P. Yu, S. Kou, Welding Research, Vol 99, 255-270, October, 2020.
3. J. C. Lippold, Welding metallurgy and weldability, First ed., M. John Wiley & Sons Inc, pp. 85-94, 2015.
4. M.C. Flemings, Solidification Processing, McGraw-Hill, New York, 1974, pp. 251-255.
5. S. A. David, C. L. White, V. P. Kujanpaa,, WELD RESEARCH SUPPLEMENT 65 (1986) 203-212.
6. K. Kadoi, A. Fujinaga, M. Yamamoto, K. Shinozaki, Weld World 57 (2013) 383-390.
7. N. N. Prokhorov, The problem of the strength of metals while solidifying during welding, Svar Proiz 6 (1956) 5-11.
8. G. J. Davies, J. G. Garland, International Materials Reviews 20 (1975) 83-108.
9. Y. Arata, F. Matsuda, S. Katayama, Transactions of JWRI 6 (1) (1997) 105-116.
10. D. Wang, K. Kadoi, K. Shinozaki, M. Yamamoto,, ISIJ International 56 (11) (2016) 2022-2028.
11. P. Wen, K. Shinozaki, M. Yamamoto, Y. Senda, T. Tamura1 and N. Nemoto, Quarterly Journal of JWS 27 (2) (2009) 134-138.
12. K. Shinozaki, M. Yamamoto, A. Kawasaki, T. Tamura, P. Wen, Materials Science Forum 580-582 (2008) 49-52.
13. J.H. Lee, S. Yamashita, T. Ogura, K. Saida, Journal of Advanced Joining Processes 3 (2021) 100044.
14. K. Shinozaki, M. Yamamoto, A. Kawazaki, T. Tamura, P. Wen, Materials Science Forum 589-582 (2008) 49–52.
15. P. Wen, M. Yamamoto, Y. Senda, T. Tamura, K. Shinozaki, Weld Word 54 (2010) 257-266.